ACS Energy LETTERS

http://pubs.acs.org/journal/aelccp

Probing the Role of Atomic Defects in Photocatalytic Systems through Photoinduced Enhanced Raman Scattering

Daniel Glass,* Raul Quesada-Cabrera, Steven Bardey, Premrudee Promdet, Riccardo Sapienza, Valérie Keller, Stefan A. Maier, Valérie Caps, Ivan P. Parkin,* and Emiliano Cortés

Cite This: *ACS Energy Lett.* 2021, 6, 4273−4281

Read Online

ACCESS | Metrics & More | Article Recommendations | Supporting Information

ABSTRACT: **Even in ultralow quantities, oxygen vacancies (V_O) drastically impact key properties of metal oxide semiconductors, such as charge transport, surface adsorption, and reactivity, playing central roles in functional materials performance. Current methods used to investigate V_O often rely on specialized instrumentation under far from ideal reaction conditions. Hence, the influence of V_O generated *in situ* during catalytic processes has yet to be probed. In this work, we assess *in situ* extrinsic surface V_O formation and lifetime under photocatalytic conditions which we compare to photocatalytic performance. We show for the first time that lifetimes of *in situ* generated atomic V_O play more significant roles in catalysis than their concentration, with strong correlations between longer-lived V_O and higher photocatalytic activity. Our results indicate that enhanced photocatalytic efficiency correlates with *goldilocks* V_O concentrations, where V_O densities must be just right to encourage carrier transport while avoiding charge carrier trapping.**

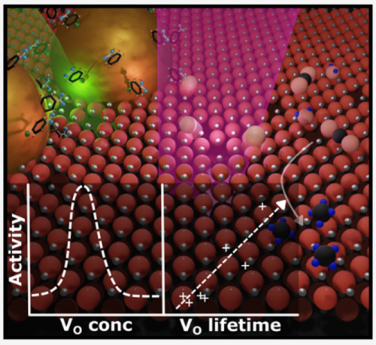

Metal oxide semiconductors (MOSs) are some of the most extensively researched materials playing a central role in the world economic market, from sensors to solar cells.[1−3] Due to their electronic structures and light absorption properties, MOS substrates are widely used in the field of photocatalysis for wastewater treatment,[4,5] environmental pollutant remediation,[5−8] and solar fuel production (water splitting,[9−12] CO_2 photoreduction[13]). MOS band structures define their ability to promote photoinduced charge transfers (PICTs) needed for photocatalytic processes. Nonetheless, for most MOSs, efficient PICTs are limited by charge carrier dynamics, drastically reducing their effective photocatalytic activity under irradiation conditions. Charge transport to active sites and carrier lifetimes are hindered by recombination processes. In the past decades, considerable efforts in material engineering have been made to improve this problem, and yet, limited efficiency and/or carrier lifetimes are still major challenges toward optimized photocatalysts for solar energy conversion.[14−17]

An interesting approach toward favorable charge transport processes follows the introduction of oxygen vacancies (V_O) within the material,[7,18−29] as desired properties of the substrate, such as toxicity and biocompatibility, are not drastically changed with partial reduction/oxidization.[7,30] V_O are some of the most common reactive defect sites in MOSs, considerably impacting material properties even in a few ppm.[31] Nevertheless, the role vacancies play in photocatalytic behavior of MOSs remains unclear in the literature, with contradictory results over their beneficial or detrimental impact.[7,19,25,26,32−35] The presence of V_O has been suggested to enhance electron donor density, improving charge carrier transport.[7,19] Local charge induced by defects can greatly influence carrier transport.[36] Furthermore, V_O create electron/hole donor levels within the MOS band gap, promoting light adsorption and charge carrier photogeneration.[18,37] On the other hand, V_O can act as recombination centers, impacting photocatalytic efficiency.[38]

The seemingly contradictory viewpoints on the role of V_O likely originate from different methods used to engineer V_O and therefore the distribution and concentrations of V_O across the subtrate.[39,40] The antagonism of surface vs bulk effects has been highlighted as one of the key outstanding challenges in photocatalysis.[41] As a general rule, bulk and surface defects act as carrier traps promoting charge recombination, whereas

Received: August 22, 2021
Accepted: October 21, 2021

https://doi.org/10.1021/acsenergylett.1c01772
ACS Energy Lett. 2021, 6, 4273−4281

surface defects can also interact with adsorbed species, preventing recombination and enhancing photocatalytic activity.

Among the many reported methods for defect engineering, photoinducing defects is a promising method to selectively create surface over bulk V_O in MOSs.[19,42−44] While photoinduced defects are often short-lived,[45] due to self-healing upon exposure to air, induced V_O remain long enough for a significant number of interactions with target molecules.[42] Photoinduced carriers localize around defect sites,[46] increasing carrier lifetimes and their chance of aiding photocatalytic processes.[44,47] In addition, V_O formation often occurs with the production of reduced metal centers, e.g., Ti^{3+} in titanium dioxide (TiO_2), which alter the local surface charge, significantly affecting the surface reactivity[48] and preferential reaction pathways.[49] Hence, there is a central need to probe defects created *in situ* under the conditions of photocatalytic processes to clarify their effect on the photocatalytic system. The access to this information can strongly impact future MOS-based photocatalytic material design.

Yet, technical limitations exist in the characterization of V_O under environments close to reaction conditions. Therefore, characterization is typically carried out *ex situ*, in the absence of illumination and usually under ultrahigh vacuum or low-temperature conditions using bulky scanning probe techniques.[50−55] Furthermore, techniques commonly use ideal single-crystal surfaces, and their conclusions may be far from those of practical polycrystalline materials. *In situ* characterization of V_O is crucial not only toward the rationale of the material performance but also to monitor V_O kinetics under reaction conditions and thus assess the role of V_O in reaction mechanisms. This is particularly relevant to photocatalytic processes, as *extrinsic* V_O may be formed under UV irradiation conditions at the MOS surface, greatly affecting photocatalytic processes.

Raman spectroscopy has been shown to be a powerful tool for *in situ* catalytic monitoring[56] and therefore is a promising approach to overcome these issues. Recently, we reported on a novel technique based on photoinduced enhanced Raman scattering (PIERS)[42,45] which has been used as an innovative tool to probe surface V_O.[42,45,57−60] In the PIERS scheme, MOS samples are pre-irradiated under high-energy UVC light (λ = 254 nm) to induce surface V_O (Scheme 1.1). The induced defects alter the local surface environment affecting the charge distribution and vibronic states of Raman probes while creating band gap states. This, in turn, allows new resonant PICT pathways between the Raman analyte-vacancy-MOS system through vibronic resonant coupling, further enhancing the SERS (surface enhanced Raman spectroscopy) signal (Scheme 1.2).[61,62] By monitoring the Raman band intensity over time, one can indirectly monitor the concentration of induced surface V_O.[42] It should be noted these surface V_O are often temporary, healing upon exposure to ambient conditions (Scheme 1.3).

In this work, two series of benchmark and modified photocatalytic materials designed for different environmental and energy applications were probed using PIERS. By choosing MOS materials with different forms and physical properties and assessing the photocatalytic activity by various methods under distinct reaction conditions, we ensure our conclusions are independent of the substrate type and test conditions. More importantly, the impact of V_O formation with other potential factors influencing the photocatalytic activity can be

Scheme 1. Schematic Figure Showing Photoinduced V_O Surface Defects Created under Photocatalytic Reaction Conditions[a]

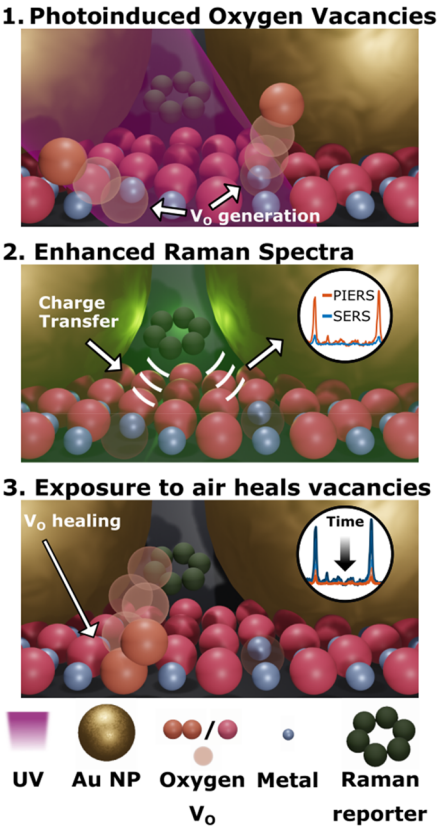

[a](1). Photoinduced V_O can interact with analyte molecules to enhance Raman spectroscopy beyond the conventional SERS intensity (2). Upon exposure to air, the generated V_O subsequently heal, eventually returning to the original SERS intensity (3). Although both V_O concentration and lifetime can greatly affect photocatalytic processes, the effects of V_O generated by irradiation during the process are largely unknown.

isolated. The induced V_O healing (V_O^-) lifetime and relative PIERS enhancement factor (EF), relating to the number of induced V_O, for each substrate was determined and correlated to their photocatalytic activity. Our results showed a strong correlation between induced vacancy lifetime and the photocatalytic response of both substrates series, signifying the correlation was independent of photocatalytic test. The PIERS enhancement against photocatalytic activity found an optimum [V_O] for photocatalytic activity for both MOS series, between high and low densities of photoinduced V_O. Our results here support the current understanding that surface defects can aid in photocatalytic activity while shedding light on the nature and importance of defects created *in situ* during photocatalytic processes. Through PIERS analysis the role and importance of V_O generated *in situ* under reaction conditions can be probed helping to understand the optimum conditions to perform photocatalytic reactions more efficiently, Scheme 1. Our results indicate the highest photocatalytic rates will be found in substrates with long induced V_O lifetimes and a "*goldilocks*" V_O concentration.

ZnO thin films and TiO_2 nanoparticles (NPs) were prepared as previously reported.[13,63] In this work, we refer to the ZnO films as **ZnO-x** and **ZnO-Ax** corresponding to the as-prepared

https://doi.org/10.1021/acsenergylett.1c01772
ACS Energy Lett. 2021, 6, 4273−4281

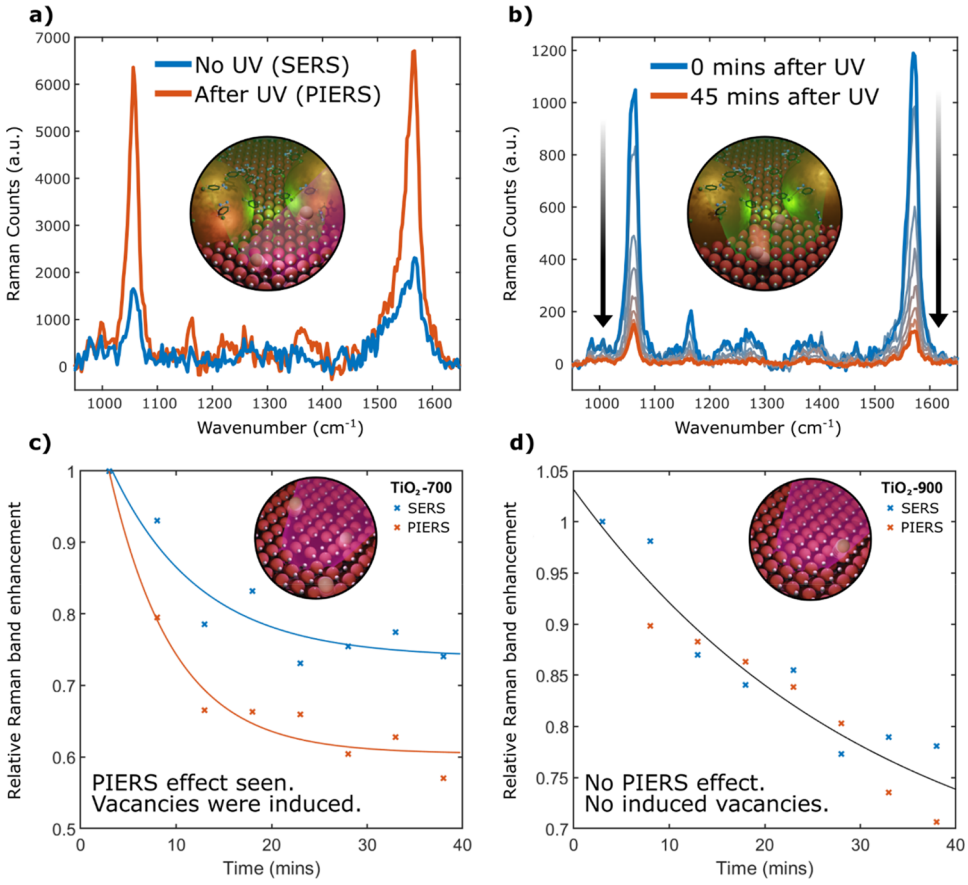

Figure 1. Sample Raman spectra for MBA functionalized AuNPs on a ZnO thin film at 3 mW excited by a He−Ne laser (633 nm) a) before (SERS) and after 1 h of 254 nm UV irradiation (PIERS) showing PIERS enhancement and b) the subsequent decrease in Raman band intensity upon exposure to air, back to the SERS background enhancement. Sample average relative SERS (no UV) and PIERS (after UV) Raman band enhancement for MBA over time relative to the initial measurement on c) TiO_2-700 and d) TiO_2-900 TiO_2 samples. Photobleaching of MBA under the Raman laser causes a decay in the SERS enhancement over time. Pre-irradiation with UV induces surface V_O (Scheme 1.1) and can form resonant charge transfer pathways enhancing the Raman band intensity beyond the conventional SERS signal (Scheme 1.2). Upon exposure to air, the generated V_O subsequently heal (Scheme 1.3), removing the enhancement pathway causing an increased relative enhancement decay. Note, an enhanced decay can be seen on TiO_2-700 between SERS and PIERS indicating significant $[V_O]$ were induced, whereas no noticeable difference is seen for TiO_2-900 indicating effectively no measurable $[V_O]$ was induced, illustrated in inset images.

and annealed films, respectively, where "x" denotes the volume of acetic acid in the precursor solution. The importance and effects of acetic acid in the solution are discussed in the Supporting Information. The TiO_2 NPs are referred to as **TiO_2**, **TiO_2-(no Au)**, and **TiO_2-y**, where **TiO_2** and **TiO_2-(no Au)** refer to the as-purchased Hombikat UV100 TiO_2 particles with and without gold nanoparticle (AuNP) loading. **TiO_2-y** refers to post-treated particles calcined and subsequently loaded with AuNPs, where **y** refers to the calcination temperature.

Structural, morphological, and functional characterization of both MOS series constitutes a fundamental step for the interpretation of the reactivity and V_O dynamics in these systems. Therefore, a detailed characterization of each sample was first performed, Supporting Information (Section 1, Figures S1−15). Prior to evaluating the photocatalytic behavior and PIERS analysis of the samples, further characterization was performed using Raman spectroscopy, Supporting Information (Section 1.2). These studies allowed for an ideal probe molecule to be identified, such that the characteristic Raman bands for the probe molecule are far from those of the respective substrates to avoid band overlap.

After characterization of the substrates, pre-functionalized AuNPs, coated with 4-mercaptobenzoic acid (MBA), were added to each sample. MBA is an attractive Raman probe molecule often used for modeling different surfaces due to its excellent Raman cross section, good water solubility, and the fact it is a polar aromatic thiol.[64] However, it is important to note the PIERS mechanism is nonspecific, so any probe analyte can be chosen. Additionally, although PIERS only requires a photocatalytic metal oxide, AuNPs were added, as they aid the PIERS process primarily in a few ways. Firstly, AuNPs can significantly contribute to the SERS enhancement by creating localized intense electromagnetic fields due to local surface plasmon resonances, a $\times 10^6$ signal enhancement or higher.[65] This aids the tracking of probe molecule band enhancements over time. Secondly, the MOS-AuNP interface creates a Schottky junction enhancing charge carrier separation which stabilizes V_O formation and reduces the V_O formation energy.[66] Finally, pre-functionalization of the Raman probe can effectively "shield" it from reactive species found on the metal oxide surface after/during UV irradiation, which can destroy the probe.[42]

https://doi.org/10.1021/acsenergylett.1c01772
ACS Energy Lett. 2021, 6, 4273−4281

Following the Raman characterization, SERS analysis was peformed, Supporting Information (Section 1.2). Characterization of the average SERS background enhancement is critical, as it serves as an effective standard for comparison of the PIERS EF and is required to determine the induced V_O^- lifetime. The PIERS analysis scheme requires determining time-dependent changes in the Raman band intensity before and after UV irradiation. In the absence of UV treatment, photobleaching effects from the Raman probe laser decrease Raman band intensities over time, referred to as a "SERS decay". To measure the SERS decay, a series of Raman spectra were first taken monitoring the relative change in MBA Raman band intensities over time at a single position on the surface. These measurements were repeated at different random positions across each respective sample to determine an average SERS decay. It should be noted that for the experimental conditions used here no evidence of MBA decarboxylation[67,68] or other competing processes was observed in any of the measured Raman series.

Additional Raman series were obtained after 1 h of high energy UVC irradiation. No significant changes were seen for substrate Raman bands for any sample. UV irradiation on photocatalytic MOSs generates photoinduced charge carriers, which can induce surface V_O.[42,45] V_O can interact with analyte molecules resulting in an increased Raman signal phenomenon, known as PIERS (Figure 1a). It is important to note that Raman analysis was conducted after the UV irradiation period such that the primary observed effects are solely due to photoinduced V_O^-.

Under ambient conditions, O_2 and H_2O in the air adsorb onto the substrate healing the induced V_O, thereby removing the enhancement pathway and lowering the Raman intensity (Figure 1b). A combination of V_O^- and laser-induced photobleaching causes an increased rate of decay of analyte band intensities over time, relative to the SERS decay. This increased decay of the Raman signal is referred to as a "PIERS decay". The background SERS enhancement is eventually reached when all induced V_O are healed.[42] An enhanced signal and increased band intensity decay rate between the PIERS and SERS decays identifies the presence of induced vacancies.

An example illustrating this procedure is shown in Figure 1c and Figure 1d, showing average relative SERS (before UV) and PIERS (after UV) enhancements over time for two TiO_2 samples. The decays are shown relative to the initial average Raman intensity to highlight the enhanced PIERS decay. Without UV treatment, a steady decrease in MBA band intensity was observed, assigned to laser-induced photobleaching effects. A noticeable difference between the SERS and PIERS relative enhancements was observed with **TiO_2-700** (Figure 1c), showing an enhanced decay after UV exposure. However, no significant difference was detected for **TiO_2-900** (Figure 1d) between the SERS and PIERS enhancements over time. This indicates that the rate of surface V_O production in **TiO_2-900** was significantly low such that effectively little (or no) V_O were induced. **TiO_2-900** was found to be highly crystalline (Figure S6) and displayed an extremely low surface area (Figure S14), which may explain the lower V_O production rate. A similar analysis was conducted for each substrate. Almost all samples were found to behave similarly to **TiO_2-700**, showing significant differences between SERS and PIERS measurements. The average PIERS EF, i.e., the average relative enhancement over the SERS background intensity which is related to the photoinduced surface V_O concentration, and induced V_O^- lifetimes could then be calculated.

The V_O^- lifetimes and average PIERS EFs for each respective sample were compared with the structural, morphological, and functional characterization of each MOS. For the ZnO series, no significant relationship or correlation was observed, Figure S16. Contrastingly, Figure S17a–d suggests an ideal calcination temperature, crystallite size, surface area, and pore volume, respectively, for longer-lived induced V_O. Photoinduced V_O heal via interactions with surface adsorbed species, such as O_2 and H_2O.[42] While an increase in calcination temperature increased the crystallite size, a decrease in surface area and pore volume was observed, Table S2. Changes in the surface area and structure affect both the mobility of adsorbed species and their concentration, explaining the observed trends. No significant relationship or correlation was observed for the PIERS EF against other material property for the TiO_2 series, Figure S17g–k.

After measuring the dynamics of photoinduced V_O on each substrate, the photocatalytic activity of each sample was evaluated. The photocatalytic activity of ZnO films was evaluated upon degradation of stearic acid under UVA irradiation, expressed in terms of formal quantum efficiency (i.e., number of molecules degraded per incident photon), Table S3. The photocatalytic activity of the TiO_2 series was evaluated upon photoreduction of CO_2 with water in the gas phase under solar irradiation, measured by the electron utilization rate (i.e., number of moles of photoinduced electrons involved in the production of CH_4 and H_2 from CO_2 and H_2O, respectively), Table S4. The photocatalytic activity was measured through different methods for each series, formal quantum efficiency (ZnO) and overall electronic activity (TiO_2), due to the different applications of each respective sample. By comparing the photocatalytic activity determined by different methods for substrates designed for different photocatalytic applications, we ensure the results are independent of the photocatalytic test and test conditions.

Many factors can affect the photocatalytic properties of a substrate, such as crystallinity, crystalline phase, specific surface area, and defect states. Figure S16m–q and Figure S17m–q compare the measures of photocatalytic activity against the structural, morphological, and functional characterization for all substrates. No significant correlation or relationship was observed between the photocatalytic behavior and the material properties for the ZnO films, Figure S16. In contrast to this, efficient photocatalytic behavior was observed with ideal calcination temperature, crystallite size, surface area, and pore volume for the TiO_2 particles, Figure S17. How each of these factors affect the photocatalytic activity for comparable systems to those studied here has been previously discussed in detail.[13,63] Due to the nature of thin films in comparison to NPs, more pronounced structural and morphological changes are observed between different TiO_2 samples than ZnO samples. This explains why no significant trend in material properties against the photocatalytic activity was observed with the ZnO series, but some trends were observed with the TiO_2 series.

In this study, we are primarily concerned about the overall metric of the photocatalytic activity and therefore have not discussed the specific effects these factors have on the photocatalytic trends measured. It is noteworthy that the mechanism for photoinduced V_O production on MOSs depends on photoinduced carrier production and interactions

https://doi.org/10.1021/acsenergylett.1c01772
ACS Energy Lett. 2021, 6, 4273−4281

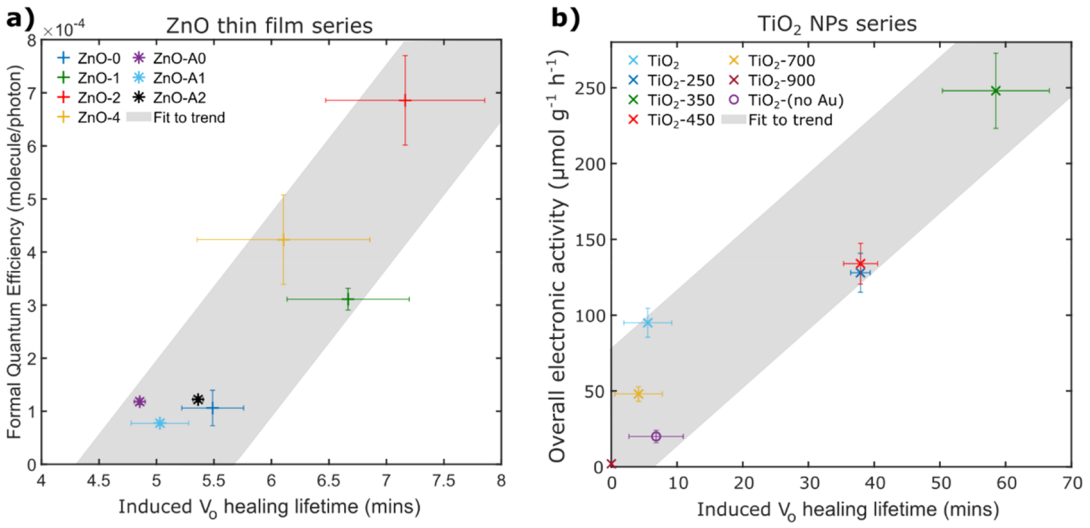

Figure 2. Calculated induced V_O healing lifetimes determined through PIERS analysis against measures of photocatalytic activity of a) a series of ZnO thin films and b) a series of TiO_2 NPs. The photoinduced V_O healing lifetime was calculated from SERS and PIERS average relative enhancements following the method previously described.[42] The photocatalytic activity of ZnO films was measured in terms of formal quantum efficiency for the degradation of stearic acid molecules. The photocatalytic activity of TiO_2 NPs was measured in terms of overall electronic activity, i.e., the mass- and time-normalized number of moles of electrons involved in the CO_2/H_2O to CH_4/H_2 reaction.

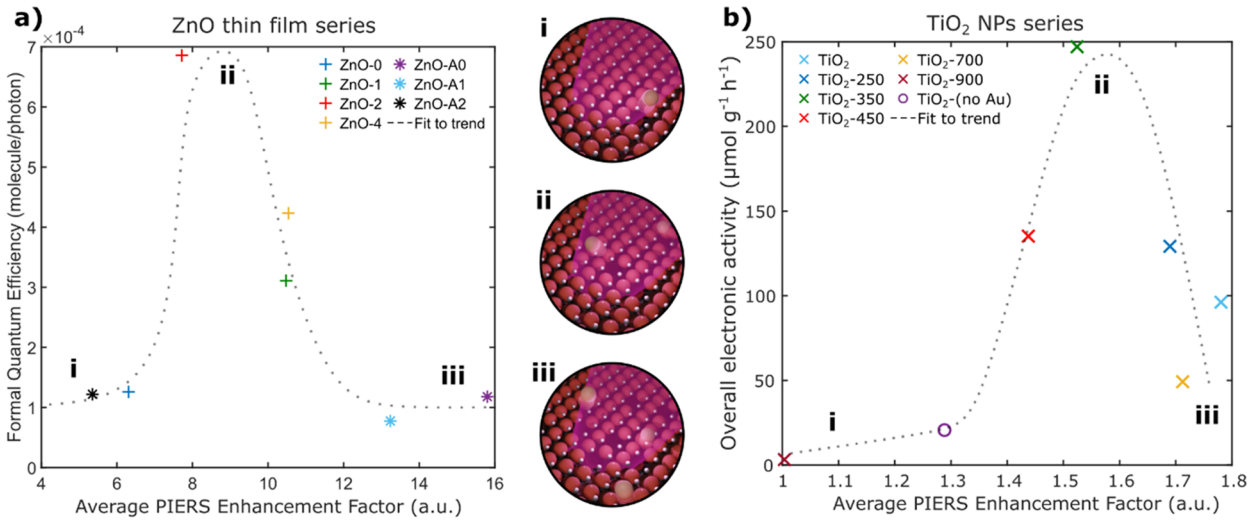

Figure 3. Measured average PIERS enhancement factor (relative enhancement over the SERS background) against measures of photocatalytic activity of a series of ZnO thin films and b) a series of TiO_2 NPs. The photocatalytic activity of ZnO films was measured in terms of formal quantum efficiency for the degradation of stearic acid molecules. The photocatalytic activity of TiO_2 NPs was measured in terms of overall electronic activity, i.e., the mass- and time-normalized number of moles of electrons involved in the CO_2/H_2O to CH_4/H_2 reaction. Dotted lines are visual guides to showing comparative trends. Positions i, ii, and iii correspond to the cases of low, medium, and high relative photoinduced $[V_O]$, as shown in the central images.

with surface adatoms.[42] Hence, it is likely the factors which affect photocatalysis will also affect PIERS. This is highlighted by the comparative features in Figure S16 and Figure S17 between V_O^- lifetimes, photocatalytic behavior, and the respective material properties.

The photocatalytic activity was then correlated with the PIERS analysis described above, i.e., V_O lifetimes and PIERS EFs. A summary of the photocatalytic activity and both the determined V_O^- lifetime and average PIERS EF is shown in Table S3 and Table S4 for the ZnO and TiO_2 series, respectively. Figure 2a and Figure 2b show the calculated induced V_O^- lifetime against the photocatalytic activity for ZnO and TiO_2 samples, respectively, showing a strong correlation for both series between the induced V_O^- lifetime and the photocatalytic activity.

We now turn to correlate the enhancement values in the PIERS signal of each sample, instead of the decay profiles. The average PIERS enhancement against the photocatalytic activity is shown in Figure 3a and Figure 3b, for ZnO and TiO_2 samples, respectively. In contrast to the V_O^- lifetime, no linear correlation was observed between photocatalytic activity and the number of induced vacancy states, as inferred from the PIERS enhancement. In general, samples that showed either negligible or very significant PIERS EFs (Figure 3 positions **i** and **iii**), corresponding to small and large induced $[V_O]$, respectively, showed poor photocatalytic performance. In between this range, substrates with modest PIERS enhance-

https://doi.org/10.1021/acsenergylett.1c01772
ACS Energy Lett. 2021, 6, 4273−4281

ment reached the greatest photocatalytic activity for both series (Figure 3 position **ii**), demonstrating a sort of "*goldilocks*" effect.

This *Gaussian*-type trend of first increased then decreased photocatalytic activity with induced [V_O] has been reported for many MOS substrates.[13,19,28,63,69−72] However, often no explanation is given for this result. We believe this can be explained by the dual nature that surface V_O play within photocatalytic processes. Trap centers, such as V_O, greatly affect carrier recombination.[38,49,73−75] On one side, surface V_O act as recombination sites ultimately lowering the photocatalytic activity. On the other hand, increased [V_O] can improve carrier transport, thereby increasing the photocatalytic activity. Once the charge carriers are initially trapped, the carriers can more effectively migrate to more stable trapping sites or participate in photocatalytic processes.[74] Surface V_O sites can act as "stepping stones", allowing induced carriers to "hop" between defects and surface trap sites.[32] Thus, initially increasing the [V_O] facilitates charge carrier separation and therefore increases the likelihood of carriers interacting with reactive species for photocatalytic processes, Figure 3 position **i**. However, after a certain threshold, Figure 3 position **ii**, a further increase in the number of V_O results in enhanced recombination, ultimately lowering the photocatalytic activity again, Figure 3 position **iii**.

Overall, the rate of carrier recombination and carrier dynamics play more significant roles in defining how good a photocatalyst the material actually is than the induced carrier concentration. Temporary V_O created *in situ* during photocatalytic processes can greatly affect them. Our results here demonstrate insight into the effect surface V_O have on photocatalytic processes, suggesting long-lived V_O states induced during photocatalytic reactions may have a larger effect on the photocatalytic activity than the number of V_O induced. Short V_O lifetimes result in rapid removal of these transport sites, inhibiting the transport and migration of charge carriers to adsorbed molecules for photocatalytic processes.

In summary, the photocatalytic activity of two MOS series, ZnO thin films and TiO_2 NPs, was compared to the calculated induced V_O^- lifetimes and the measured average PIERS EF, proportional to the induced [V_O]. These results showed a strong correlation between the atomic V_O^- lifetimes and the photocatalytic activity, where longer lived V_O resulted in higher substrate photocatalytic activity. Low photocatalytic activity was found to correspond with samples with small PIERS enhancements. Increasing the PIERS EF initially resulted in better photocatalytic production; however, at large induced [V_O], the photocatalytic activity was found to reduce again. These observations can be understood through the dual processes in which surface V_O play in photocatalytic processes, both in charge carrier recombination and transportation. Surface V_O can greatly aid in charge carrier transport while acting as trap sites which increases carrier lifetimes. Hence, substrates which produce longer lived V_O may facilitate more photocatalytic reactions. However, our results also suggest an ideal photocatalyst should be tuned to allow neither large nor small photoinduced [V_O]. This work marks an important step toward characterizing atomic defects created under *in situ* photocatalytic conditions on practical substrates and their effects on photocatalytic processes. While these studies primarily focus on V_O on MOS substrates, this technique can be directly applied to different systems, for example 2D materials, to assist in understanding the role and dynamics of atomic surface defects.

■ ASSOCIATED CONTENT

Supporting Information

The Supporting Information is available free of charge at https://pubs.acs.org/doi/10.1021/acsenergylett.1c01772.

Structural, morphological, and optical characterization (including Raman and SERS) characterization of substrates; summary and comparison of substrate characterization; and comparison between material properties and values determined through PIERS analysis and photocatalytic behavior; experimental methods (PDF)

■ AUTHOR INFORMATION

Corresponding Authors

Daniel Glass − *The Blackett Laboratory, Department of Physics, Imperial College London, London SW7 2AZ, U.K.; Department of Chemistry, University College London, London WC1H 0AJ, U.K.;* orcid.org/0000-0002-5219-4148; Email: d.glass17@imperial.ac.uk

Ivan P. Parkin − *Department of Chemistry, University College London, London WC1H 0AJ, U.K.;* orcid.org/0000-0002-4072-6610; Email: i.p.parkin@ucl.ac.uk

Authors

Raul Quesada-Cabrera − *Department of Chemistry, University College London, London WC1H 0AJ, U.K.; Fotoelectrocatálisis para Aplicaciones Medioambientales (FEAM), Departamento de Química, Universidad de Las Palmas de Gran Canaria (ULPGC), Las Palmas de Gran Canaria 35017, Spain*

Steven Bardey − *Institut de Chimie et Procédés pour l'Energie, l'Environnement et la Santé (ICPEES), CNRS UMR 7515, Université de Strasbourg, 67087 Strasbourg, France*

Premrudee Promdet − *Department of Chemistry, University College London, London WC1H 0AJ, U.K.;* orcid.org/0000-0002-4509-523X

Riccardo Sapienza − *The Blackett Laboratory, Department of Physics, Imperial College London, London SW7 2AZ, U.K.;* orcid.org/0000-0002-4208-0374

Valérie Keller − *Institut de Chimie et Procédés pour l'Energie, l'Environnement et la Santé (ICPEES), CNRS UMR 7515, Université de Strasbourg, 67087 Strasbourg, France;* orcid.org/0000-0002-3381-1446

Stefan A. Maier − *The Blackett Laboratory, Department of Physics, Imperial College London, London SW7 2AZ, U.K.; Chair in Hybrid Nanosystems, Faculty of Physics, Ludwig Maximilians Universität München, 80539 München, Germany;* orcid.org/0000-0001-9704-7902

Valérie Caps − *Institut de Chimie et Procédés pour l'Energie, l'Environnement et la Santé (ICPEES), CNRS UMR 7515, Université de Strasbourg, 67087 Strasbourg, France;* orcid.org/0000-0001-9330-2566

Emiliano Cortés − *Chair in Hybrid Nanosystems, Faculty of Physics, Ludwig Maximilians Universität München, 80539 München, Germany;* orcid.org/0000-0001-8248-4165

Complete contact information is available at: https://pubs.acs.org/10.1021/acsenergylett.1c01772

Notes

The authors declare no competing financial interest.

■ ACKNOWLEDGMENTS

D.G. acknowledges funding from the UK MOD for the Ph.D. under contract DSTLX-1000116630. S.A.M. and E.C. acknowledge funding and support from the Deutsche Forschungsgemeinschaft (DFG, German Research Foundation) under Germany's Excellence Strategy − EXC 2089/1-390776260, the Bavarian program Solar Energies Go Hybrid (SolTech), and the Center for NanoScience (CeNS). S.A.M. additionally acknowledges the Lee-Lucas Chair in Physics. E.C. acknowledges the European Commission through the ERC Starting Grant CATALIGHT (802989). P.P acknowledges funding from The Development and Promotion of Science and Technology Talents Project. S.B., V.K., and V.C. acknowledge funding and support from IFP Energies Nouvelles. I.P.P acknowledges support from the EPSRC Centre of Doctoral Training in Molecular Modelling and Material Science under grant EP/L015862/1. R.Q.C. would like to thank the Beatriz Galindo Program, Ministerio de Educación y Formación Profesional, Spain. The authors also acknowledge support from EPSRC - UK under the grant EP/M013812/1, Reactive Plasmonics.

■ REFERENCES

(1) Zaleska-Medynska, A. *Metal Oxide-Based Photocatalysis: Fundamentals and Prospects for Application*; Korotcenkov, G., Ed.; Elsevier: 2018; DOI: 10.1016/C2016-0-01872-7.

(2) Danish, M. S. S.; Bhattacharya, A.; Stepanova, D.; Mikhaylov, A.; Grilli, M. L.; Khosravy, M.; Senjyu, T. A Systematic Review of Metal Oxide Applications for Energy and Environmental Sustainability. *Metals (Basel, Switz.)* **2020**, *10* (12), 1604.

(3) Suzuki, S.; Fukui, K. I.; Onishi, H.; Iwasawa, Y. Hydrogen Adatoms on TiO2(110)-(1 × 1) Characterized by Scanning Tunneling Microscopy and Electron Stimulated Desorption. *Phys. Rev. Lett.* **2000**, *84* (10), 2156.

(4) Liu, Y.; Chen, X.; Li, J.; Burda, C. Photocatalytic Degradation of Azo Dyes by Nitrogen-Doped TiO2nanocatalysts. *Chemosphere* **2005**, *61* (1), 11−18.

(5) Carp, O.; Huisman, C. L.; Reller, A. Photoinduced Reactivity of Titanium Dioxide. *Prog. Solid State Chem.* **2004**, *32*, 33.

(6) Zhou, Y.; Zhang, Z.; Fang, Z.; Qiu, M.; Ling, L.; Long, J.; Chen, L.; Tong, Y.; Su, W.; Zhang, Y.; Wu, J. C. S.; Basset, J. M.; Wang, X.; Yu, G. Defect Engineering of Metal-Oxide Interface for Proximity of Photooxidation and Photoreduction. *Proc. Natl. Acad. Sci. U. S. A.* **2019**, *116* (21), 10232−10237.

(7) Bai, S.; Zhang, N.; Gao, C.; Xiong, Y. Defect Engineering in Photocatalytic Materials. *Nano Energy* **2018**, *53*, 296−336.

(8) Hurum, D. C.; Agrios, A. G.; Gray, K. A.; Rajh, T.; Thurnauer, M. C. Explaining the Enhanced Photocatalytic Activity of Degussa P25 Mixed-Phase TiO $_2$ Using EPR. *J. Phys. Chem. B* **2003**, *107* (19), 4545−4549.

(9) Soltani, T.; Tayyebi, A.; Lee, B. K. Sonochemical-Driven Ultrafast Facile Synthesis of WO3 Nanoplates with Controllable Morphology and Oxygen Vacancies for Efficient Photoelectrochemical Water Splitting. *Ultrason. Sonochem.* **2019**, *50*, 230.

(10) Song, H.; Li, C.; Lou, Z.; Ye, Z.; Zhu, L. Effective Formation of Oxygen Vacancies in Black TiO2 Nanostructures with Efficient Solar-Driven Water Splitting. *ACS Sustainable Chem. Eng.* **2017**, *5* (10), 8982−8987.

(11) Lei, F.; Sun, Y.; Liu, K.; Gao, S.; Liang, L.; Pan, B.; Xie, Y. Oxygen Vacancies Confined in Ultrathin Indium Oxide Porous Sheets for Promoted Visible-Light Water Splitting. *J. Am. Chem. Soc.* **2014**, *136*, 6826.

(12) Tang, J.; Durrant, J. R.; Klug, D. R. Mechanism of Photocatalytic Water Splitting in TiO2. Reaction of Water with Photoholes, Importance of Charge Carrier Dynamics, and Evidence for Four-Hole Chemistry. *J. Am. Chem. Soc.* **2008**, *130* (42), 13885−13891.

(13) Bardey, S.; Bonduelle-Skrzypczak, A.; Fécant, A.; Cui, Z.; Colbeau-Justin, C.; Caps, V.; Keller, V. Plasmonic Photocatalysis Applied to Solar Fuels. *Faraday Discuss.* **2019**, *214*, 417−439.

(14) Qian, R.; Zong, H.; Schneider, J.; Zhou, G.; Zhao, T.; Li, Y.; Yang, J.; Bahnemann, D. W.; Pan, J. H. Charge Carrier Trapping, Recombination and Transfer during TiO2 Photocatalysis: An Overview. *Catal. Today* **2019**, *335*, 78−90.

(15) Chen, R.; Fan, F.; Dittrich, T.; Li, C. Imaging Photogenerated Charge Carriers on Surfaces and Interfaces of Photocatalysts with Surface Photovoltage Microscopy. *Chem. Soc. Rev.* **2018**, *47* (22), 8238−8262.

(16) Bai, S.; Jiang, J.; Zhang, Q.; Xiong, Y. Steering Charge Kinetics in Photocatalysis: Intersection of Materials Syntheses, Characterization Techniques and Theoretical Simulations. *Chem. Soc. Rev.* **2015**, *44* (10), 2893−2939.

(17) Zhang, P.; Wang, T.; Chang, X.; Gong, J. Effective Charge Carrier Utilization in Photocatalytic Conversions. *Acc. Chem. Res.* **2016**, *49* (5), 911−921.

(18) Xiong, L. B.; Li, J. L.; Yang, B.; Yu, Y. Ti 3+ in the Surface of Titanium Dioxide: Generation, Properties and Photocatalytic Application. *J. Nanomater.* **2012**, *2012*, 831524.

(19) Pan, X.; Yang, M.-Q.; Fu, X.; Zhang, N.; Xu, Y.-J. Defective TiO2 with Oxygen Vacancies: Synthesis, Properties and Photocatalytic Applications. *Nanoscale* **2013**, *5* (9), 3601.

(20) Greiner, M. T.; Chai, L.; Helander, M. G.; Tang, W.-M.; Lu, Z.-H. Transition Metal Oxide Work Functions: The Influence of Cation Oxidation State and Oxygen Vacancies. *Adv. Funct. Mater.* **2012**, *22* (21), 4557−4568.

(21) Tuller, H. L.; Bishop, S. R. Point Defects in Oxides: Tailoring Materials Through Defect Engineering. *Annu. Rev. Mater. Res.* **2011**, *41* (1), 369−398.

(22) Ganduglia-Pirovano, M. V.; Hofmann, A.; Sauer, J. Oxygen Vacancies in Transition Metal and Rare Earth Oxides: Current State of Understanding and Remaining Challenges. *Surf. Sci. Rep.* **2007**, *62* (6), 219−270.

(23) Elbanna, O.; Fujitsuka, M.; Kim, S.; Majima, T. Charge Carrier Dynamics in TiO2Mesocrystals with Oxygen Vacancies for Photocatalytic Hydrogen Generation under Solar Light Irradiation. *J. Phys. Chem. C* **2018**, *122* (27), 15163−15170.

(24) Hoch, L. B.; Szymanski, P.; Ghuman, K. K.; Hea, L.; Liao, K.; Qiao, Q.; Reyes, L. M.; Zhu, Y.; El-Sayed, M. A.; Singh, C. V.; Ozin, G. A. Carrier Dynamics and the Role of Surface Defects: Designing a Photocatalyst for Gas-Phase CO2 Reduction. *Proc. Natl. Acad. Sci. U. S. A.* **2016**, *113* (50), E8011−E8020.

(25) Xiao, Z.; Huang, Y.-C.; Dong, C.-L.; Xie, C.; Liu, Z.; Du, S.; Chen, W.; Yan, D.; Tao, L.; Shu, Z.; Zhang, G.; Duan, H.; Wang, Y.; Zou, Y.; Chen, R.; Wang, S. Operando Identification of the Dynamic Behavior of Oxygen Vacancy-Rich Co 3 O 4 for Oxygen Evolution Reaction. *J. Am. Chem. Soc.* **2020**, *142*, 12087−12095.

(26) Chen, H.; Wu, T.; Li, X.; Lu, S.; Zhang, F.; Wang, Y.; Zhao, H.; Liu, Q.; Luo, Y.; Asiri, A. M.; Feng, Z.-S.; Zhang, Y.; Sun, X. Modulating Oxygen Vacancies of TiO 2 Nanospheres by Mn-Doping to Boost Electrocatalytic N 2 Reduction. *ACS Sustainable Chem. Eng.* **2021**, *9*, 1512−1517.

(27) Hüttenhofer, L.; Eckmann, F.; Lauri, A.; Cambiasso, J.; Pensa, E.; Li, Y.; Cortés, E.; Sharp, I. D.; Maier, S. A. Anapole Excitations in Oxygen-Vacancy-Rich TiO2- x Nanoresonators: Tuning the Absorption for Photocatalysis in the Visible Spectrum. *ACS Nano* **2020**, *14* (2), 2456−2464.

(28) Liu, H.; Mei, H.; Miao, N.; Pan, L.; Jin, Z.; Zhu, G.; Gao, J.; Wang, J.; Cheng, L. Synergistic Photocatalytic NO Removal of Oxygen Vacancies and Metallic Bismuth on Bi12TiO20 Nanofibers under Visible Light Irradiation. *Chem. Eng. J.* **2021**, *414*, 128748.

https://doi.org/10.1021/acsenergylett.1c01772
ACS Energy Lett. 2021, 6, 4273−4281

(29) Khalil, I. E.; Xue, C.; Liu, W.; Li, X.; Shen, Y.; Li, S.; Zhang, W.; Huo, F. The Role of Defects in Metal−Organic Frameworks for Nitrogen Reduction Reaction: When Defects Switch to Features. *Adv. Funct. Mater.* **2021**, *31*, 2010052.
(30) Schweke, D.; Mordehovitz, Y.; Halabi, M.; Shelly, L.; Hayun, S. Defect Chemistry of Oxides for Energy Applications. *Adv. Mater.* **2018**, *30*, 1706300.
(31) Gunkel, F.; Christensen, D. V.; Chen, Y. Z.; Pryds, N. Oxygen Vacancies: The (in)Visible Friend of Oxide Electronics. *Appl. Phys. Lett.* **2020**, *116* (12), 120505.
(32) Grad, L.; Novotny, Z.; Hengsberger, M.; Osterwalder, J. Influence of Surface Defect Density on the Ultrafast Hot Carrier Relaxation and Transport in Cu2O Photoelectrodes. *Sci. Rep.* **2020**, *10* (1), 10686.
(33) Jiang, X.; Zhang, Y.; Jiang, J.; Rong, Y.; Wang, Y.; Wu, Y.; Pan, C. Characterization of Oxygen Vacancy Associates within Hydrogenated TiO2: A Positron Annihilation Study. *J. Phys. Chem. C* **2012**, *116* (42), 22619−22624.
(34) Hu, J.; Yu, L.; Deng, J.; Wang, Y.; Cheng, K.; Ma, C.; Zhang, Q.; Wen, W.; Yu, S.; Pan, Y.; Yang, J.; Ma, H.; Qi, F.; Wang, Y.; Zheng, Y.; Chen, M.; Huang, R.; Zhang, S.; Zhao, Z.; Mao, J.; Meng, X.; Ji, Q.; Hou, G.; Han, X.; Bao, X.; Wang, Y.; Deng, D. Sulfur Vacancy-Rich MoS2 as a Catalyst for the Hydrogenation of CO2 to Methanol. *Nat. Catal.* **2021**, *4* (3), 242−250.
(35) Yu, F.; Wang, C.; Li, Y.; Ma, H.; Wang, R.; Liu, Y.; Suzuki, N.; Terashima, C.; Ohtani, B.; Ochiai, T.; Fujishima, A.; Zhang, X. Enhanced Solar Photothermal Catalysis over Solution Plasma Activated TiO2. *Adv. Sci.* **2020**, *7* (16), 2000204.
(36) Hill, J. W.; Hill, C. M. Directly Visualizing Carrier Transport and Recombination at Individual Defects within 2D Semiconductors. *Chem. Sci.* **2021**, *12*, 5102−5112.
(37) Jing, L.; Xin, B.; Yuan, F.; Xue, L.; Wang, B.; Fu, H. Effects of Surface Oxygen Vacancies on Photophysical and Photochemical Processes of Zn-Doped TiO2 Nanoparticles and Their Relationships. *J. Phys. Chem. B* **2006**, *110* (36), 17860−17865.
(38) Deák, P.; Aradi, B.; Frauenheim, T. Quantitative Theory of the Oxygen Vacancy and Carrier Self-Trapping in Bulk TiO2. *Phys. Rev. B: Condens. Matter Mater. Phys.* **2012**, *86* (19), 1−8.
(39) Nam, Y.; Li, L.; Lee, J. Y.; Prezhdo, O. V. Strong Influence of Oxygen Vacancy Location on Charge Carrier Losses in Reduced TiO2 Nanoparticles. *J. Phys. Chem. Lett.* **2019**, *10*, 2676−2683.
(40) Kong, M.; Li, Y.; Chen, X.; Tian, T.; Fang, P.; Zheng, F.; Zhao, X. Tuning the Relative Concentration Ratio of Bulk Defects to Surface Defects in TiO2 Nanocrystals Leads to High Photocatalytic Efficiency. *J. Am. Chem. Soc.* **2011**, *133* (41), 16414−16417.
(41) Ohtani, B. Photocatalysis A to Z-What We Know and What We Do Not Know in a Scientific Sense. *J. Photochem. Photobiol., C* **2010**, *11*, 157−178.
(42) Glass, D.; Cortés, E.; Ben-Jaber, S.; Brick, T.; Peveler, W. J. W. J.; Blackman, C. S. C. S.; Howle, C. R.; Quesada-Cabrera, R.; Parkin, I. P. I. P.; Maier, S. A. S. A. Dynamics of Photo-Induced Surface Oxygen Vacancies in Metal-Oxide Semiconductors Studied Under Ambient Conditions. *Adv. Sci.* **2019**, *6* (22), 1901841.
(43) Hensling, F. V. E.; Keeble, D. J.; Zhu, J.; Brose, S.; Xu, C.; Gunkel, F.; Danylyuk, S.; Nonnenmann, S. S.; Egger, W.; Dittmann, R. UV Radiation Enhanced Oxygen Vacancy Formation Caused by the PLD Plasma Plume. *Sci. Rep.* **2018**, *8*, 8846.
(44) Berger, T.; Sterrer, M.; Diwald, O.; Knözinger, E.; Panayotov, D.; Thompson, T. L.; Yates, J. T. Light-Induced Charge Separation in Anatase TiO 2 Particles. *J. Phys. Chem. B* **2005**, *109* (13), 6061−6068.
(45) Ben-Jaber, S.; Peveler, W. J.; Quesada-Cabrera, R.; Cortés, E.; Sotelo-Vazquez, C.; Abdul-Karim, N.; Maier, S. A.; Parkin, I. P. Photo-Induced Enhanced Raman Spectroscopy for Universal Ultra-Trace Detection of Explosives, Pollutants and Biomolecules. *Nat. Commun.* **2016**, *7*, 12189.
(46) Liu, B.; Zhao, X.; Yu, J.; Parkin, I. P.; Fujishima, A.; Nakata, K. Intrinsic Intermediate Gap States of TiO2Materials and Their Roles in Charge Carrier Kinetics. *J. Photochem. Photobiol., C* **2019**, *39*, 1−57.
(47) Schneider, J.; Matsuoka, M.; Takeuchi, M.; Zhang, J.; Horiuchi, Y.; Anpo, M.; Bahnemann, D. W. Understanding TiO2 Photocatalysis: Mechanisms and Materials. *Chem. Rev.* **2014**, *114* (19), 9919−9986.
(48) Wang, R.; Hashimoto, K.; Fujishima, A.; Chikuni, M.; Kojima, E.; Kitamura, A.; Shimohigoshi, M.; Watanabe, T.; Fujishima, A.; Wang, R.; Hashimoto, K.; Watanabe, T.; Chikuni, M.; Kojima, E.; Kitamura, A.; Shimohigoshi, M. Photogeneration of Highly Amphiphilic TiO 2 Surfaces. *Adv. Mater.* **1998**, *10* (2), 135−138.
(49) Papageorgiou, A. C.; Beglitis, N. S.; Pang, C. L.; Teobaldi, G.; Cabailh, G.; Chen, Q.; Fisher, A. J.; Hofer, W. A.; Thornton, G. Electron Traps and Their Effect on the Surface Chemistry of TiO2(110). *Proc. Natl. Acad. Sci. U. S. A.* **2010**, *107* (6), 2391−2396.
(50) Bikondoa, O.; Pang, C. L.; Ithnin, R.; Muryn, C. A.; Onishi, H.; Thornton, G. Direct Visualization of Defect-Mediated Dissociation of Water on TiO 2(110). *Nat. Mater.* **2006**, *5* (3), 189−192.
(51) Lindan, P. J. D.; Harrison, N. M.; Gillan, M. J. Mixed Dissociative and Molecular Adsorption of Water on the Rutile (110) Surface. *Phys. Rev. Lett.* **1998**, *80* (4), 762−765.
(52) Kurtz, R. L.; Stock-Bauer, R.; Msdey, T. E.; Román, E.; De Segovia, J. L. Synchrotron Radiation Studies of H2O Adsorption on TiO2(110). *Surf. Sci.* **1989**, *218* (1), 178−200.
(53) Mezhenny, S.; Maksymovych, P.; Thompson, T. L.; Diwald, O.; Stahl, D.; Walck, S. D.; Yates, J. T. STM Studies of Defect Production on the TiO2(110)-(1 × 1) and TiO2(110)-(1 × 2) Surfaces Induced by UV Irradiation. *Chem. Phys. Lett.* **2003**, *369* (1−2), 152−158.
(54) Lun Pang, C.; Lindsay, R.; Thornton, G. Chemical Reactions on Rutile TiO 2 (110). *Chem. Soc. Rev.* **2008**, *37*, 2328−2353.
(55) Enevoldsen, G. H.; Foster, A. S.; Christensen, M. C.; Lauritsen, J. V.; Besenbacher, F. Noncontact Atomic Force Microscopy Studies of Vacancies and Hydroxyls of TiO2(110): Experiments and Atomistic Simulations. *Phys. Rev. B: Condens. Matter Mater. Phys.* **2007**, *76* (20), 205415.
(56) Hess, C. New Advances in Using Raman Spectroscopy for the Characterization of Catalysts and Catalytic Reactions. *Chem. Soc. Rev.* **2021**, *50*, 3519−3564.
(57) Zhao, J.; Wang, Z.; Lan, J.; Khan, I.; Ye, X.; Wan, J.; Fei, Y.; Huang, S.; Li, S.; Kang, J. Recent Advances and Perspectives in Photo-Induced Enhanced Raman Spectroscopy. *Nanoscale* **2021**, *13*, 8707−8721.
(58) Barbillon, G.; Noblet, T.; Humbert, C. Highly Crystalline ZnO Film Decorated with Gold Nanospheres for PIERS Chemical Sensing. *Phys. Chem. Chem. Phys.* **2020**, *22*, 21000−21004.
(59) Zhang, M.; Chen, T.; Liu, Y.; Zhu, J.; Liu, J.; Wu, Y. Three-Dimensional TiO 2 -Ag Nanopore Arrays for Powerful Photoinduced Enhanced Raman Spectroscopy (PIERS) and Versatile Detection of Toxic Organics. *ChemNanoMat* **2019**, *5* (1), 55.
(60) Almohammed, S.; Zhang, F.; Rodriguez, B. J.; Rice, J. H. Photo-Induced Surface-Enhanced Raman Spectroscopy from a Diphenylalanine Peptide Nanotube-Metal Nanoparticle Template. *Sci. Rep.* **2018**, *8* (1), 41−44.
(61) Wang, X.; Shi, W.; Wang, S.; Zhao, H.; Lin, J.; Yang, Z.; Chen, M.; Guo, L. Two-Dimensional Amorphous TiO2 Nanosheets Enabling High-Efficiency Photoinduced Charge Transfer for Excellent SERS Activity. *J. Am. Chem. Soc.* **2019**, *141* (14), 5856−5862.
(62) Alessandri, I.; Lombardi, J. R. Enhanced Raman Scattering with Dielectrics. *Chem. Rev.* **2016**, *116* (24), 14921−14981.
(63) Promdet, P.; Quesada-Cabrera, R.; Sathasivam, S.; Li, J.; Jiamprasertboon, A.; Guo, J.; Taylor, A.; Carmalt, C. J.; Parkin, I. P. High Defect Nanoscale ZnO Films with Polar Facets for Enhanced Photocatalytic Performance. *ACS Appl. Nano Mater.* **2019**, *2* (5), 2881−2889.
(64) Bell, S. E. J.; Charron, G.; Cortøs, E.; Kneipp, J.; Lamy De La Chapelle, M.; Langer, J.; Arek Prochμzka, M.; Tran, V.; Schlücker, S. Towards Reliable and Quantitative Surface-Enhanced Raman Scattering (SERS): From Key Parameters to Good Analytical Practice. *Angew. Chem., Int. Ed.* **2020**, *59*, 5454−5462.
(65) Maier, S. A. *Plasmonics: Fundamentals and Applications*; Springer: 2007; DOI: 10.1007/0-387-37825-1.

https://doi.org/10.1021/acsenergylett.1c01772
ACS Energy Lett. 2021, 6, 4273−4281

(66) Ruiz Puigdollers, A.; Schlexer, P.; Tosoni, S.; Pacchioni, G. Increasing Oxide Reducibility: The Role of Metal/Oxide Interfaces in the Formation of Oxygen Vacancies. *ACS Catal.* **2017**, *7*, 6493.
(67) Zhang, Q.; Chen, K.; Wang, H. Hot-Hole-Induced Molecular Scissoring: A Case Study of Plasmon-Driven Decarboxylation of Aromatic Carboxylates. *J. Phys. Chem. C* **2021**, *125* (38), 20958−20971.
(68) Huang, S. C.; Wang, X.; Zhao, Q. Q.; Zhu, J. F.; Li, C. W.; He, Y. H.; Hu, S.; Sartin, M. M.; Yan, S.; Ren, B. Probing Nanoscale Spatial Distribution of Plasmonically Excited Hot Carriers. *Nat. Commun.* **2020**, *11* (1), 4211.
(69) Xia, T.; Zhang, Y.; Murowchick, J. Vacuum-Treated Titanium Dioxide Nanocrystals: Optical Properties, Surface Disorder, Oxygen Vacancy, and Photocatalytic Activities. *Catal. Today* **2014**, *225*, 2−9.
(70) Li, D.; Haneda, H.; Labhsetwar, N. K.; Hishita, S.; Ohashi, N. Visible-Light-Driven Photocatalysis on Fluorine-Doped TiO 2 Powders by the Creation of Surface Oxygen Vacancies. *Chem. Phys. Lett.* **2005**, *401* (4−6), 579−584.
(71) Qi, W.; Zhang, F.; An, X.; Liu, H.; Qu, J. Oxygen Vacancy Modulation of {010}-Dominated TiO2for Enhanced Photodegradation of Sulfamethoxazole. *Catal. Commun.* **2019**, *118*, 35.
(72) Xiao, F.; Zhou, W.; Sun, B.; Li, H.; Qiao, P.; Ren, L.; Zhao, X. Engineering Oxygen Vacancy on Rutile TiO 2 for Efficient Electron-Hole Separation and High Solar-Driven Photocatalytic Hydrogen Evolution. *Sci. CHINA Mater.* **2018**, *61* (6), 822.
(73) Li, J.; Zhang, M.; Guan, Z.; Li, Q.; He, C.; Yang, J. Synergistic Effect of Surface and Bulk Single-Electron-Trapped Oxygen Vacancy of TiO2 in the Photocatalytic Reduction of CO2. *Appl. Catal., B* **2017**, *206*, 300.
(74) Yang, S.; Brant, A. T.; Halliburton, L. E. Photoinduced Self-Trapped Hole Center in TiO2 Crystals. *Phys. Rev. B: Condens. Matter Mater. Phys.* **2010**, *82* (3), 035209.
(75) Zhou, Z.; Liu, J.; Long, R.; Li, L.; Guo, L.; Prezhdo, O. V. Control of Charge Carriers Trapping and Relaxation in Hematite by Oxygen Vacancy Charge: Ab Initio Non-Adiabatic Molecular Dynamics. *J. Am. Chem. Soc.* **2017**, *139* (19), 6707−6717.

https://doi.org/10.1021/acsenergylett.1c01772
ACS Energy Lett. 2021, 6, 4273−4281